Effect of temperature on the creep behavior of a Ni–Cr–Fe–Al alloy: a comparison of the experimental data and a model

Essam El-Magd · Jürgen Gebhard · Jan Stuhrmann

Abstract In order to characterise the mechanical behaviour of sandwich structures, which combine an interlayer of a woven wire mesh between two thin walled sheet metals, creep tests at 650, 680 and 750 °C were carried out on sheet metals made of the nickel based alloy Nicrofer 6025 HT (2.4633). In addition to the tests the creep behaviour was simulated by a model, which considers the creep rate as a function of the applied stress σ and the internal deformation resistance including an internal back stress σ_i and a particle resistance σ_P. The damage is included by a damage parameter D, which converges to ''one'' with increasing damage. A concluding comparison with the creep test results shows that the model is able to describe the creep behaviour of the investigated sheet metals.

Introduction

This study is carried out in the frame of the collaborative Research program ''Thermally Highly Loaded, Porous and Cooled Multi-Layer Systems for Combined Cycle Power Plants'' of the University of Aachen. The goal is to increase the efficiency in combined cycle power plants from 58% up to 65% during the next 25 years. In order to obtain higher efficiency in the modern combined cycle power plants temperature and pressure have to be increased. To achieve steam operating temperatures around 680 °C and steam pressures about 350 bar a new lay out of steam turbines is necessary.

In a preliminary investigation a cooling system was developed which combines an interlayer of a woven wire mesh between two plane face sheets. This sandwich structure designated as a facing for the steam turbine casing and the rotor enables cooling steam to pass without severe losses. Figure 1 shows a schematic drawing of the structure and its application in the steam turbine [1].
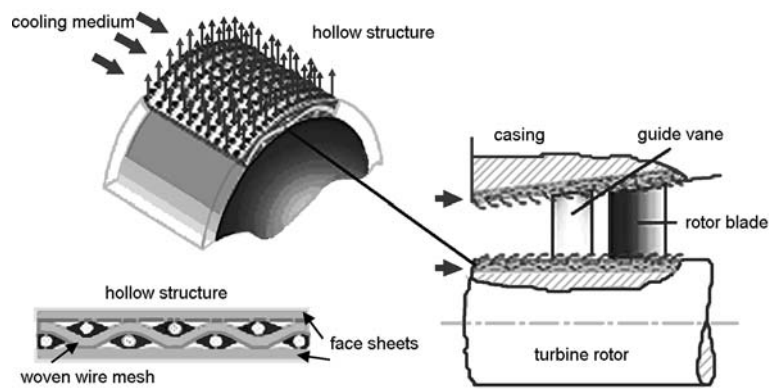
Current developments of 9–12% chromium steels, such as P92, have sufficient oxidation resistance in steam and good creep resistance up to approximately 600 °C [2]. For higher temperatures it is necessary to use nickel based alloys, such as Nicrofer 6025HT. Since this material has been brought onto the marked in the year 1992 the popularity increased rapidly in many application areas such as kiln engineering, automotive and chemicals industry [3–5].

In order to characterise and simulate the mechanical behaviour of the sandwich structure under high temperature loads, it is necessary to investigate the properties of its constituents for the first instance. Especially an exact knowledge of the creep behaviour of the Nicrofer 6025HT sheet metals is essential for an accurate prediction of the failure behaviour under service conditions of the so called Grid-Sheet structures.

Furthermore the obtained results are required on the one hand for constitutive equations implemented in numerical simulations and on the other hand for a comparison to the mechanical properties of thick-walled bulk material for instance piping. Constitutive equations based on a combination of overstress and threshold stress concept allow an adequate description of the creep behaviour if successive damage is taken into consideration.

E. El-Magd · J. Gebhard · J. Stuhrmann (✉)
Lehr- und Forschungsgebiet Werkstoffkunde RWTH Aachen,
Augustinerbach 4, 52062 Aachen, Germany
e-mail: Jan.Stuhrmann@iwk.rwth-aachen.de

Fig. 1 The new cooling concept of the rotor and the housing surfaces

Test material: Nicrofer 6025HT

This material is a high-carbonaceous nickel–chromium–iron alloy with alloying additions of titanium, zirconium, aluminium and yttrium. The chemical composition is given in Table 1. Nicrofer 6025 HT is characterised by great high-temperature creep strength. The grain size of the microstructure can be set by different solution annealing temperatures. Optimal properties concerning the creep behaviour can be achieved by a solution temperature of 1220 °C leading to a grain size greater than 70 μm. Solution annealing at 1170 °C produces a finer grain-sized microstructure (30–60 μm) and due to this increased low cycle fatigue behaviour [6]. The carbide diameter is in the range 5–10 μm.

The high oxidation resistance, even under extreme conditions like cyclic heating-up and cooling-down, is achieved by a close adhering aluminium oxide layer. Additionally the high chromium concentration leads to a remarkable oxidation resistance in sulfureous atmospheres.

In this work the cold rolled sheets (thickness 1 mm) with a cold deformation of 65% were solution annealed in a continuous annealing furnace at approximately 1170 °C for 2 min followed by solution annealing in a vacuum furnace at 1220 °C for 1 h and cooled in nitrogen with a cooling rate of approximately 10 K/min.

The microstructure of the investigated material is shown in Fig. 2. The grain size was measured and found around 80 μm whereas much smaller grains are existent. The Vickers hardness value at room temperature for the material averages 197HV10. Nicrofer 6025HT is hardened by solid solution and carbide strengthening. Due to the high carbon concentration concerning nickel based alloys in addition to approximately 25% Cr primary $Cr_{23}C_6$-carbides are

precipitated and distributed homogeneously in the microstructure as well as on the grain boundaries. As a result of their remarkable high thermal stability the primary $Cr_{23}C_6$-carbides are operative up to working temperatures of 1250 °C [7].

Creep model

In addition to testing the creep behaviour of the sheet metals was investigated experimentally, this behaviour was predicted by the so called concept of the internal backstress.

The current value of strain rate depends on the current values of applied stress σ, internal back stress σ_i, particle deformation resistance σ_P, material creep resistance σ_F and degree of damage D. The creep rate can be described by a modified power law [8–11]:

$$\dot{\varepsilon} = A \left[\frac{\sigma - (\sigma_i + \sigma_P)}{\sigma_F(1 - D)} \right]^n \tag{1}$$

where in case of high-temperature creep

$$A = \dot{\varepsilon}_0 \exp\left(-\frac{Q}{RT}\right) \text{ with } Q = 2.9\text{E5} \frac{\text{kJ}}{\text{kmol}}$$
$$\text{and } R = 8.3141 \frac{\text{kJ}}{\text{kmol K}} \tag{2}$$

In this equitation Q is the activation energy for self diffusion of the base material and $\dot{\varepsilon}_0$ is a constant.

According to [12] the evolution of the internal back stress σ_i is given by

$$\frac{d\sigma_i}{d\varepsilon} = \frac{C_1}{\varepsilon_s}(\sigma_{is} - \sigma_i) \tag{3}$$

Table 1 Chemical composition of Nicrofer 6025HT (2.4633) in percent by weight

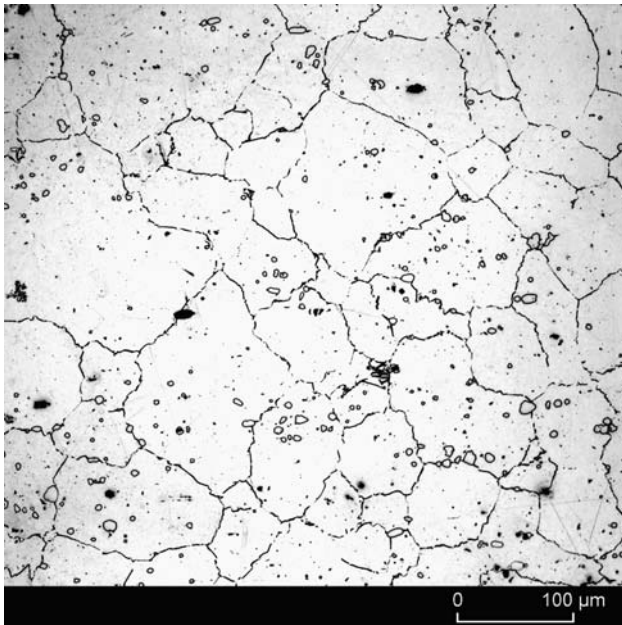| Ni	Cr	Fe	C	Al	Ti	Zr	Y
Rest	24.0–26.0	8.0–11.0	0.15–0.25	1.8–2.4	0.1–0.2	0.01–0.10	0.05–0.12

Fig. 2 Microstructure of Nicrofer 6025HT

and validated experimentally in [13]. In Eq. 3, σ_{is} is the quasi-stationary value of the internal back stress, ε_s is the creep strain at the end of the primary creep stage and C_1 is a constant. σ_{is} can be calculated according to

$$\frac{\sigma_{is}}{\sigma_{iss}} = \frac{\sigma}{\sigma_{iss}}\left[1 - \frac{\kappa}{N}\left(\frac{N-\kappa}{N}\frac{\sigma}{\sigma_{iss}}\right)^{\frac{N}{\kappa}-1}\right]; \text{ for } \sigma/\sigma_{iss} < N/(N-\kappa) \tag{4}$$

where N is the Norton–Bailey stress exponent and κ a parameter which can be set equal to 4 [14]. For different stresses the quasi-stationary value σ_{is} reaches a temperature dependent saturation value σ_{iss}. In this work the approximation

$$\sigma_{iss} \approx 1.4 R_{m/1000} \tag{5}$$

has been used [12].

The variation of σ_p with creep time is given by the relationship

$$\frac{\sigma_P}{\sigma_{P_{max}}} = \left[\frac{1+a}{1+a\left(\frac{t}{t^*}\right)^{-\upsilon}}\right]^{m/2}\left(\frac{t}{t^*}\right)^{-1/\mu} \tag{6}$$

where $a = \frac{2}{m\upsilon\mu-2}$. In Eq. 6, t^* is the point of time at the minimum creep rate when σ_p reaches its maximum value $\sigma_{P_{max}}$. For practical applications, some of the material parameters can be set equal to certain values. Assuming that ripening takes place on the basis of volume diffusion, the parameter μ is to be set equal to 3. Furthermore, the variation of the volume fraction of the precipitation with

time can be well described with $m = 2$ as far as the parameter υ can be determined from the best fit of the experimental results [12].

According to [14], $\sigma_{P_{max}}$ can be written as a function of the applied stress σ minus the quasi-stationary value of the internal back stress σ_{is} as

$$\sigma_{P_{max}} = C_4(\sigma - \sigma_{is})^{n_4} \tag{7}$$

where C_4 an n_4 are constants.

Damage as a function of creep strain according to Kachanov and Rabotnov [15, 16] modified by [17] (Eq. 8) has been used in the model:

$$D = 1 - \left(1 - \frac{\varepsilon}{\varepsilon_F}\right)^{m_D} \tag{8}$$

In this equation ε_F is the strain to rupture and m_D a material parameter.

Creep test results

Creep tests at temperatures of 650, 680 and 750 °C have been carried out on Nicrofer 6025HT sheet metals. In Fig. 3(a) the minimal creep rate $\dot{\varepsilon}_{min}$ is plotted as a function of the applied stress σ and described by the Norton–Bailey equation $\dot{\varepsilon}_{min} = B(T) \cdot \sigma^N$. As shown in Fig. 3(b) the Norton–Bailey exponent N decreases with an increase of the applied test temperature. Due to enhanced precipitations at 680 °C which influence the creep mechanism a minor decrease of the exponent N was observed in the range of 680–750 °C.

Figure 4 shows the applied stress plotted against the time to rupture up to 1000 h creep life. As expected the creep strength decreases with increasing temperature. The
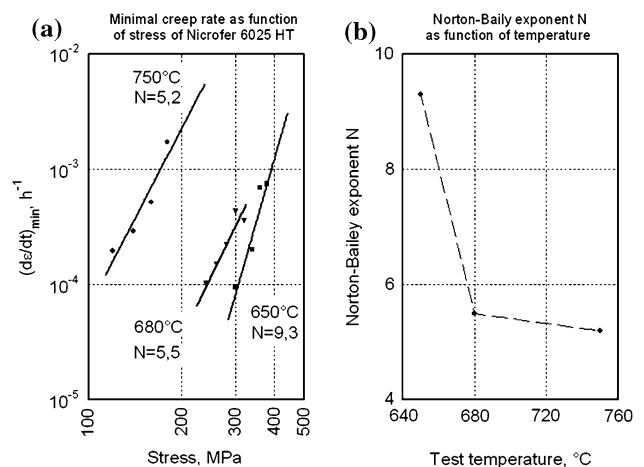

Fig. 3 (**a**) Minimal creep rate versus stress. (**b**) Norton-Bailey exponent as function of temperature
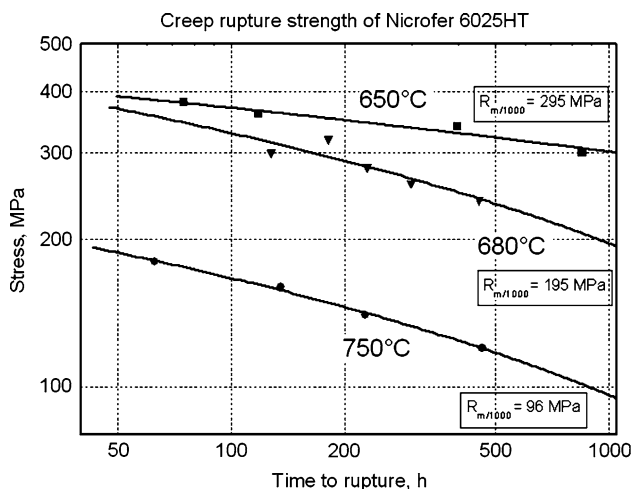
Fig. 4 Creep rupture time versus stress for Nicrofer 6025HT

obtained stress values for a creep life of 1000 h are 295, 195 and 96 MPa for 650, 680 and 750 °C, respectively.

The obtained values for N and $R_{m/1000}$ have been used to calculate the quasi-stationary value of σ_{is}.

Application of the model to creep tests

Figures 5–7 show a comparison between the creep test results (markers) and the predictions of the model (curves) for temperatures of 650, 680 and 750 °C. Each Figure is divided into two diagrams designated with (a) and (b). In case of (a) the creep strain over time and in case of (b) the creep rate over time are plotted for four different applied test stresses. Although relatively rough approximations have been used the model leads to an acceptable description of the experimental data.

Figures 8 (a), (b) and 9 (a), (b) present the dependency of the used model parameters on the stress for the corre-
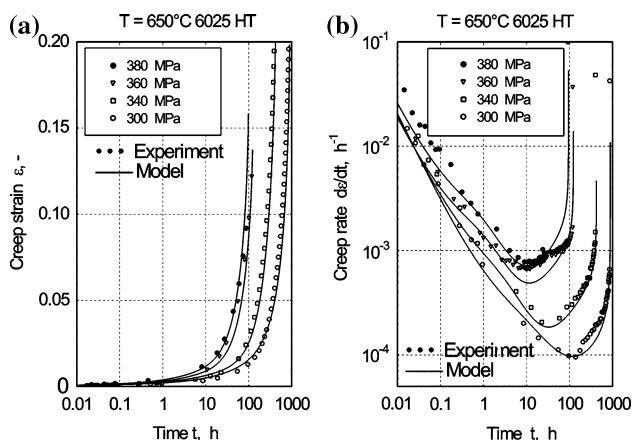

Fig. 5 Comparison between test results and predictions of model at $T = 650$ °C (**a**) Creep strain versus time (**b**) Creep rate versus time
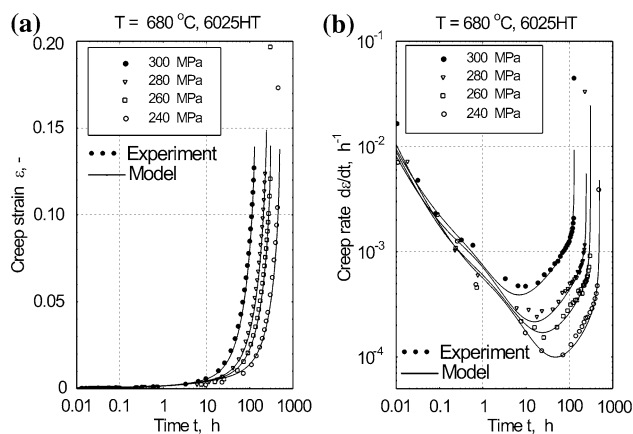

Fig. 6 Comparison between test results and predictions of model at $T = 680$ °C (**a**) Creep strain versus time (**b**) Creep rate versus time
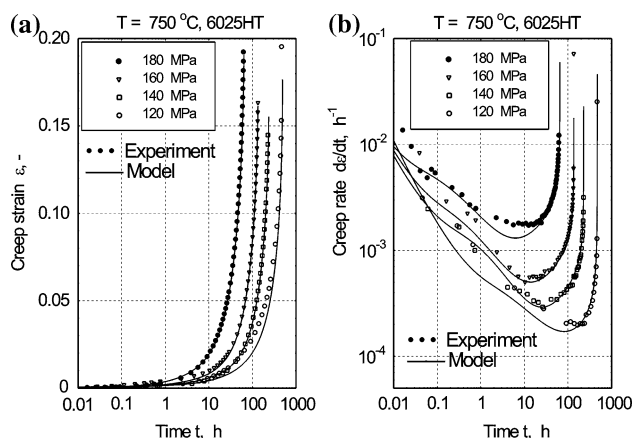

Fig. 7 Comparison between test results and predictions of model at $T = 750$ °C (**a**) Creep strain versus time (**b**) Creep rate versus time
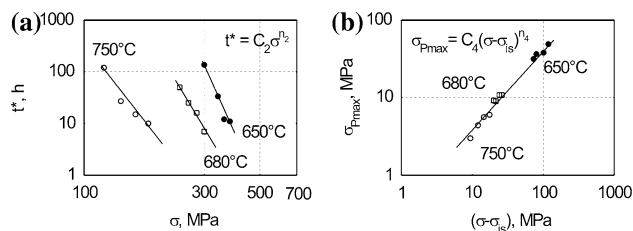

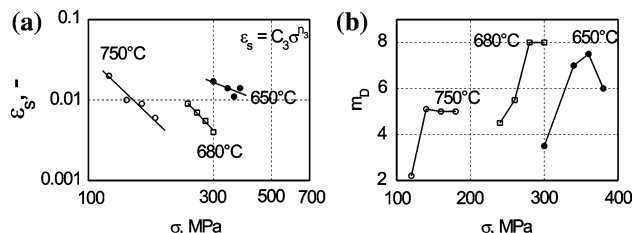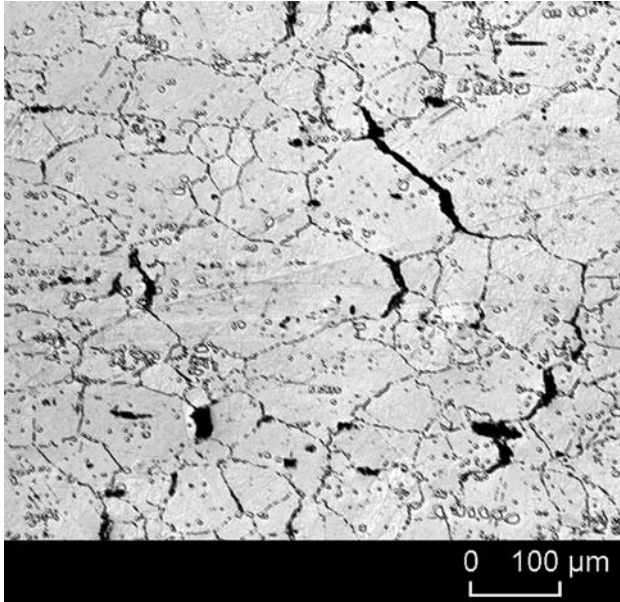**Fig. 8** (**a**) Dependency of the model parameter t^* on the stress (**b**) Dependency of the model parameter σ_{Pmax} on the stress

Fig. 9 (**a**) Dependency of the model parameter ε_s on the stress (**b**) Dependency of the model parameter m_D on the stress

Table 2 Parameters of the model

T	$\dot{\varepsilon}_0$	C_1	n	C_2	n_2	C_3	n_3	v	m_D	ε_F
650 °C	7.7E5	30	4	1E29	–10.8	26.9	–1.3	0.7–1	3.5–7	0.16–0.21
680 °C	5.5E7	40	4	1E21	–8.11	1.47E6	–3.45	0.8	4.5–8	0.14–0.15
750 °C	5.5E7	80	4	1E15	–6.23	5.8E4	–3.12	0.7	2.2–5.1	0.16–0.19

Fig. 10 Microstructure close to the fracture zone of the material tested at 750 °C and 140 MPa

sponding test temperatures. The parameters t*, ε_s and $\sigma_{P_{max}}$ were described by power functions shown in Figs. 8 (a), (b) and 9(a) as well.

Table 2 gives a summary of the parameters used for the model. According to the test temperatures the parameters C_4 and n_4 have been optimised to 0.374 and 1.01.

Due to differing influence of precipitation hardening during the creep tests the parameter $\dot{\varepsilon}_0$ deviates in case of 650 °C from $\dot{\varepsilon}_0$ at 680 °C and 750 °C. The lower test temperature of 650 °C retards the initiation of precipitations and affects the creep behaviour significant.

The damage exponent m_D takes the minimum values in case of the lowest stress values at each temperature. A low value of m_D describes a constant increase of damage within creep time. In Fig. 10 the microstructure of a fractured test specimen is shown. The material fails according to Zener-mechanism at grain boundary triple points (wedge-type cracks) [18] where stress concentration leading to crack initiation takes place. With increasing stress, crack growth rate increases leading to a spontaneous fracture of the complete specimen and thus to a major value of m_D.

Reference

1. Dilthey U, Hachmann B, Kopp R,Marek U, Rappen J (1994) VDI-Berichte 1080, 657
2. Wachter O, Ennis PJ (1997) VGB Kraftwerkstechnik 77(9)
3. Brill U, Giersbach G, Kettler H-W (1995) Effizienzsteigerung kontinuierlicher Wärmebehandlungsanlagen durch den Einsatz ungekühlter Ofenrollen aus dem neuen Werkstoff Nicrofer 6025 HT (2.4633), VDI-Berichte Nr. 1151
4. Brill U (1995) Praktische Erfahrungen mit dem neuen Werkstoff Nicrofer 6025 HT im Ofen- und Wärmebehandlungsanlagenbau. Verlag Stahleisen GmbH, Düsseldorf, pp 37–40
5. Brill U (1999) Ergebnisse mit dem Werkstoff Nicrofer 6025 HT im Ofen- und Wärmebehandlungsanlagenbau. Verlag Stahleisen GmbH, Düsseldorf, pp 54–56
6. Werkstoffdatenblatt Nicrofer 6025H/HT-alloy 602/602 CA, Werkstoffdatenblatt Nr. 4137, Thyssen Krupp VDM GmbH, (2000)
7. Eigenschaften und Einsatzgebiete der neuen warmfesten Legierung Nicrofer 6025 HT, Zeitschrift Stahl, Verlag Stahleisen GmbH, Düsseldorf, (1994), 32–35
8. El-Magd E, Nicolini G, Farag MM (1996) Metall Trans A 27A(3):747
9. Dünnwald J, El-Magd E (1996) Comput Mater Sci 7S:200
10. Dünnwald J, El-Magd E, Deuper M, Löchte L, Gottstein G (1997). Betrachtung der Ausscheidungskinetik in Al–Cu–Mg (AA2024). mit äußerer Spannung sowie deren Auswirkung auf das Kriechverhalten,Werkstoffwoche 1996 in Stuttgart, Tagungsband zu Symposium 7 „Materialwissenschaftliche Grundlagen'', DGM-Verlag S. 23–28
11. El-Magd E, Shaker C (1991) Z. Werkstofftech 22(2S):56
12. El-Magd E (2004) In: Totten GE, Xie L, Funatani K (eds) Modeling and simulation for material selection and mechanical design. Marcel Dekker, Inc., New York, pp 95–300
13. Wilshire B, Evans RW (eds) (1990) Creep and fracture of engineering materials and structures. The Institute of Metals, London, S. 119–129
14. Kranz, Ansgar (2002) Mechanisches Hochtemperaturverhalten der Aluminiumlegierung AA2024 in Abhängigkeit vom Umformprozess und Wärmebehandlungszustand, Dr.-Ing.-Dissertation, RWTH Aachen 03.05.
15. Kachanov LM (1967) In: Kennedy AJ (Engl. Transl. ed) The theory of creep (Teoriya polzuchesti (1960)). National lending library for science and technology, England
16. Rabotnov YN (1969) In: Leckie FA (Engl. Transl. ed) Creep problems in structural members. North Holland Publishing Company, Amsterdam, London
17. Ashby MF, Dyson BF (1984) Creep damage mechanics and micromechanics, Report DMA (A) 77 National Physical Laboratory, Teddington, England, März
18. Zener C (1948) The micro-mechanism of fracture, Fracturing of metals. American society for Metals, Cleveland/Ohio, pp 3–31